

Article

Hexogen Coating Kinetics with Polyurethane-Based Hydroxyl-Terminated Polybutadiene (HTPB) Using Infrared Spectroscopy

Heri Budi Wibowo ^{1,*} , Hamonangan Rekso Diputro Sitompul ¹ , Rika Suwana Budi ¹, Kendra Hartaya ¹, Luthfia Hajar Abdillah ¹, Retno Ardianingsih ¹ and Ratih Sanggra Murti Wibowo ²

¹ Research Organization of Aeronautics and Space—National Research and Innovation Agency (BRIN), Jakarta 13220, Indonesia; hamonanganrs@gmail.com (H.R.D.S.); sbudirika@yahoo.com (R.S.B.); kendra19838@yahoo.co.id (K.H.); luhaabdillah@gmail.com (L.H.A.); re_ardian@yahoo.com (R.A.)

² Faculty of Engineering, Universitas Gadjah Mada, Jl. Grafika No. 2 Kampus UGM, Yogyakarta 55281, Indonesia; mratihh@gmail.com

* Correspondence: heribw@gmail.com; Tel.: +62-021-4892802

Abstract: The kinetics of hexogen coating with polyurethane-based hydroxyl-terminated polybutadiene (HTPB) using infrared spectrometry was investigated. The kinetics model was evaluated through reaction steps: (1) hydroxyl and isocyanate to produce urethane, (2) urethane and isocyanate to produce allophanate, and (3) nitro and isocyanate to produce diazene oxide and carbon dioxide. HTPB, ethyl acetate, TDI (toluene diisocyanate), and hexogen were mixed for 60 min at 40 °C. The sample was withdrawn and analyzed with infrared spectroscopy every ten minutes at reference wavelengths of 2270 (the specific absorption for isocyanate groups) and 1768 cm⁻¹ (the specific absorption for N=N groups). The solvent was vaporized; then, the coated hexogen was cured in the oven for 7 days at 60 °C. The effect of temperature on the coating kinetics was studied by adjusting the reaction temperature at 40, 50, and 60 °C. This procedure was repeated with IPDI (isophorone diisocyanate) as a curing agent. The reaction rate constant, k_3 , was calculated from an independent graphic based on increasing diazene oxide concentration every ten minutes. The reaction rate constants, k_1 and k_2 , were numerically calculated using the Newton–Raphson and Runge–Kutta methods based on decreasing isocyanate concentrations. The activation energy of those steps was 1178, 1021, and 912 kJ mole⁻¹. The reaction rate of hexogen coating with IPDI was slightly faster than with TDI.

Keywords: kinetic; polyurethane; hexogen; coating



Citation: Wibowo, H.B.; Sitompul, H.R.D.; Budi, R.S.; Hartaya, K.; Abdillah, L.H.; Ardianingsih, R.; Wibowo, R.S.M. Hexogen Coating Kinetics with Polyurethane-Based Hydroxyl-Terminated Polybutadiene (HTPB) Using Infrared Spectroscopy. *Polymers* **2022**, *14*, 1184. <https://doi.org/10.3390/polym14061184>

Academic Editors: Leyre Pérez-Álvarez and Tobias Bensselfelt

Received: 18 February 2022

Accepted: 11 March 2022

Published: 16 March 2022

Publisher's Note: MDPI stays neutral with regard to jurisdictional claims in published maps and institutional affiliations.



Copyright: © 2022 by the authors. Licensee MDPI, Basel, Switzerland. This article is an open access article distributed under the terms and conditions of the Creative Commons Attribution (CC BY) license (<https://creativecommons.org/licenses/by/4.0/>).

1. Introduction

Hexogen is a highly explosive material. Hexogen is widely used as an additive to increase the combustion energy of rocket composite propellants [1,2]. The modern composite propellant has at least ammonium perchlorate (AP) as an oxidizer, aluminum as solid fuel, and hydroxyl-terminated polybutadiene (HTPB) as a binder. HTPB is a polybutadiene resin copolymerized with a diisocyanate compound to form a polyurethane binder. Hexogen has a highly mechanical sensitivity and is incompatible with HTPB binders; thus, the composite propellant manufacturing process becomes unsafe [3–5]. In order to reduce its sensitivity and agglomerations in the manufacturing of propellants [6–8], hexogen has been coated with polyurethane. However, the reported thickness of the polyurethane layer is still thick, twice the original size. Polyurethane is a non-energetic binder with low combustion energy. Therefore, it needs to be used as little as possible in propellant formulations [9,10]. As layer thickness is linear to the polyurethane concentration, the polyurethane layer should be as thin as possible.

Coating kinetics is needed to determine the coated concentration and depth of coating. Hexogen is an aromatic compound with three nitro groups. Meanwhile, polyurethane

is a polymer compound with a chain of urethane groups, and HTPB is a polybutadiene compound consisting of a butadiene group chain with a hydroxyl group at the end of the chain. Coated hexogen with polyurethane occurs due to the reaction of the nitro group of hexogen with the isocyanate group of polyurethane to form a diazene oxide group [6,7]. Polyurethane itself is produced by the reaction of di-alcohol with diisocyanate. The isocyanate group can react with the urethane group to form an allophanate group during the polymerization process. Thus, there will be a competitive reaction of isocyanates with diols to form polyurethanes, polyurethanes to form allophanates, and nitro to form diazene oxides. The reaction kinetics model must include all the reaction processes that occur.

The reaction kinetics of polyurethane-based HTPB and TDI has been widely studied based on the reaction between their functional groups. Many studies report the kinetics of polyurethane formation in bulk condition based on the change of polymer product properties such as viscosity [11–16], polymer weight [12,13], torque [17,18], thermal properties [15,18–20], and infrared spectroscopy [19–21]. Moreover, polyurethane formation in bulk and solution conditions has also been reported from the analysis of characteristic functional group changes based on infrared absorption data [22,23], viscosity change (rheology) [11–16], magnetic resonance/NMR [24,25], and heat flux [18,26]. Further, polymerization of polyurethane formation from HTPB with IPDI has also been conducted in both bulk and solution conditions [18,20,26–33]. The polymerization consists of several steps involving two hydroxyl groups in HTPB and two isocyanate groups. The polymerization will be terminated if all functional groups have reacted to form urethane groups. Ajithkumar et al. state that urethane groups can react with isocyanate groups to form allophanate groups as a branching reaction in the presence of excessive isocyanate [15,21]. In addition, Wibowo et al. also state that the linear and branching reaction could occur simultaneously and competitively [3,21]. The polymerization kinetics model can be measured using infrared spectrometry from decreasing isocyanate groups concentration with absorptions characteristic at 2270–2276 cm^{-1} . Although the infrared spectrometry method is cheap, fast, and accurate, the reaction of nitro with isocyanates to form diazene oxide compounds has never been carried out using this method. Nonetheless, studies propose that the presence of diazene oxide groups can be distinguished from nitro compounds through infrared absorption at wavelengths of 1648 and 1758–1768 cm^{-1} [34,35]. The absorption is strong enough to be a differentiator with nitro groups at the wavelength of 1300–1500 cm^{-1} , which has much interference.

This paper studied the reaction kinetics of hexogen coating with polyurethane-based HTPB using infrared spectrometry. The quantitative analysis was based on the absorbance of isocyanate and diazene oxide as reference. The diisocyanate materials used were TDI (toluene diisocyanate) and IPDI (isophorone diisocyanate). The reaction mechanism included a competitive reaction of isocyanate with a di-alcohol from HTPB, a urethane group from polyurethane, and a nitro group from a hexogen.

2. Materials and Methods

2.1. Materials

Hexogen with a particle size of approximately 100 microns was supplied by Dahana, Co., Ltd., Indonesia. Ethyl acetate p.a. was produced by Merck, and HTPB and TDI were supplied by Dalian, Co., Ltd., Dalian, China. HTPB had a hydroxyl number of 40, average functionality of 1.9, and an average molecular weight of 3000 g/mole. Meanwhile, TDI had a 2,4- to 2,6- isomers molar ratio of 80:20, and the isocyanate value was 39 mg eq/g KOH.

2.2. Instrumentations

The isocyanate and diazene oxide concentrations were measured using an infrared spectrometer FTIR (Fourier transform infrared) Hitachi IR-Prestige Serial A210043 with a standard liquid cuvet. A qualitative analysis of the isocyanate and diazene oxide concentrations was carried out by plotting the measured absorbance at wavelengths of

2265–2270 cm^{-1} and 1780 cm^{-1} to their calibration curve. The coating depth was measured with the scanning electron microscope (SEM) Phenom Word ProX Desktop [36,37].

2.3. Procedure

The calibration curve of the isocyanates concentration was performed by dissolving 0.1 g toluene diisocyanate (TDI) in 100 mL benzene. Approximately 10 mL of the solution was collected and analyzed with FTIR using a standard 10 mL cuvet. This procedure was repeated with 0.2, 0.3, and 0.4 until 1.0 mL of TDI. The measured absorbance of spectra at the wavelength of 2276 cm^{-1} was plotted to their concentration to create the calibration curve of isocyanate concentration. The diazene oxide concentration calibration curve was performed by dissolving 0.1 g 4,4'-dimethoxyazoxybenzene in the 100 mL benzene. Approximately 10 mL of the solution was extracted and analyzed with FTIR using a standard 10 mL cuvet. This procedure was repeated with 0.2, 0.3, and 0.4 until 1.0 mL of TDI. The measured absorbance of spectra at the wavelength of 1870 cm^{-1} was plotted to their concentration to create the calibration curve of diazene oxide concentration.

In the next step, 4 mL HTPB, 50 mL ethyl acetate, and TDI with an NCO to OH molar ratio of 1:1 (RNCO/OH) were poured in the 500 mL beaker glass. Two hundred grams of hexogen were added and mixed for 60 min at 40 °C. Approximately 1 mL of the sample was collected and dissolved in 100 mL of benzene every ten minutes. Ten milliliters of the sample solution was poured into the cuvet and analyzed with infrared spectroscopy. The infrared absorption peaks at wavelengths of 2270 cm^{-1} (the specific absorption for isocyanate groups) [38–40] and 1768 cm^{-1} (the specific absorption for N=N groups) [34,35] were taken as a reference. The slurry was stirred vigorously, and then the ethyl acetate was removed by vacuum drying at 50 °C for one hour. The coated hexogen was cured in the oven for 7 days at 60 °C. The coated hexogen was sieved with a 100 micron sieve. This particle size and the coating depth were measured with SEM using the watershed segmentation method to separate particles that stick or were close together [41].

The temperature effect on the coating kinetics was studied by adjusting the reaction temperature at 40, 50, and 60 °C. This procedure was repeated with IPDI as a curing agent.

The absorption of infrared spectra at a wavelength of 2267 cm^{-1} was plotted to an isocyanate calibration curve to meet the isocyanate concentration. Meanwhile, the absorption of infrared spectra at a wavelength of 1870 cm^{-1} was plotted to a diazene oxide calibration curve to meet the diazene oxide concentration.

2.4. Kinetics Model

In the coating of hexogen with polyurethane-based HTPB, the hexogen with nitro functional groups was bonded with isocyanate groups from TDI and polyurethane [34,35]. Polyurethane was produced by copolymerization of HTPB and TDI [3,11,19]. The HTPB and TDI could copolymerize through the reaction of hydroxyl groups and isocyanate groups to produce linear urethane groups as illustrated in Figure 1. Every urethane compound contained two active functional groups (i.e., isocyanate or hydroxyl) that reacted to produce new urethane groups. The urethane groups would grow to produce longer urethane chains. The urethane group also reacted with a diisocyanate to produce new linear urethane groups or branching allophanate groups. This polymerization occurred by the linear or branching reaction. The copolymerization kinetics of HTPB and TDI were simplified by the reaction of their functional groups (i.e., hydroxyl and isocyanate) because the functional group reactivity was not affected by their molecular size [3]. The newest copolymerization kinetics approach of HTPB and TDI proposed a linear reaction of hydroxyl functional groups and isocyanate functional groups to produce urethane groups (Equation (1)) and a branching reaction of urethane functional groups and isocyanate groups to produce allophanate groups (Equation (2)) [3,17,42,43]. The reaction of HTPB and TDI occurred through linear and branch bond formation [3,11,15,23].

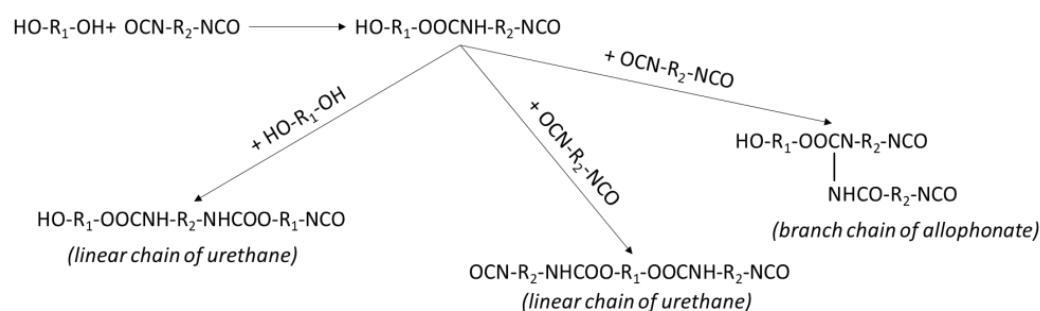
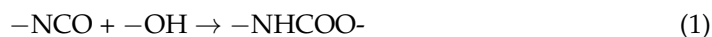


Figure 1. The copolymerization mechanism of diol (HTPB) and diisocyanate (TDI).

The kinetics model based on the hydroxyl groups from HTPB (A) reacting with isocyanate groups from TDI (B) produced urethane groups (D) via linear bonding. The urethane groups (D) then reacted with other isocyanate groups (B) to produce allophanate groups (E) via branch bonding. The reactions were expressed in Equations (1) and (2). The isocyanate groups (B) also reacted with a nitro group (F) in hexogen to produce diazene oxide groups (G) and carbon dioxide (H) [29]. The reaction was expressed in Equation (3). In the coating of hexogen, there were competitive reactions involving the isocyanate with hydroxyl groups of HTPB, urethane groups of polyurethane, and nitro groups of the hexogen.



3. Results and Discussion

3.1. Coated Hexogen Identification

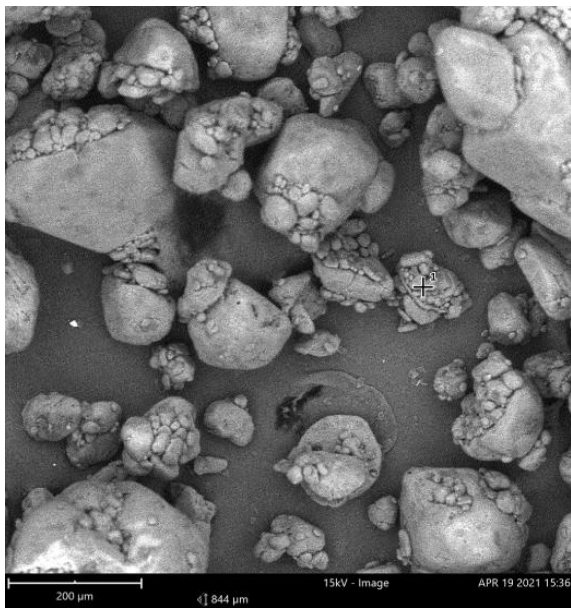
The change in particle size and shape parameters indicated the coated hexogen as illustrated in Figure 2. The average particle size of hexogen decreased from 127.68 to 96.85 microns (hexogen PU-coated with IPDI) and 64.08 microns (hexogen PU-coated with TDI) refers to Table 1. The homogenization effect due to the dispersion in ethyl acetate solution could explain this size reduction phenomenon in which the hexogen particle breaks down in size before reacting with coating substances [44,45]. Besides the particle size, the spherical shape increased from 0.78 to 0.87 (circularity) and from 0.71 to 0.78 (roundness) using IPDI as isocyanates in PU coating. In contrast, the particle size reduction was more significant using TDI. The shape parameters, such as circularity were unchanged, yet the roundness and aspect ratio was worse than the uncoated particle. These results were similar to the hexogen coating with HTPB-based polyurethane carried out by Neudorfl et al. [34,35]. The coated hexogen was more spherical than pure hexogen. Circularity is a shape descriptor that could mathematically imply the level of similarity to a perfect circle. A circularity score of 1.0 classified a perfect circle. As the circularity value reached 0.0, the shape was an increasing number much less circular. Roundness was similar to circularity. However, it was insensitive to abnormal borders alongside the fringe of the foramen. Roundness also considers the substantial axis of the exceptional suit ellipse [46].

Table 1. Comparison between uncoated and coated hexogen particles.

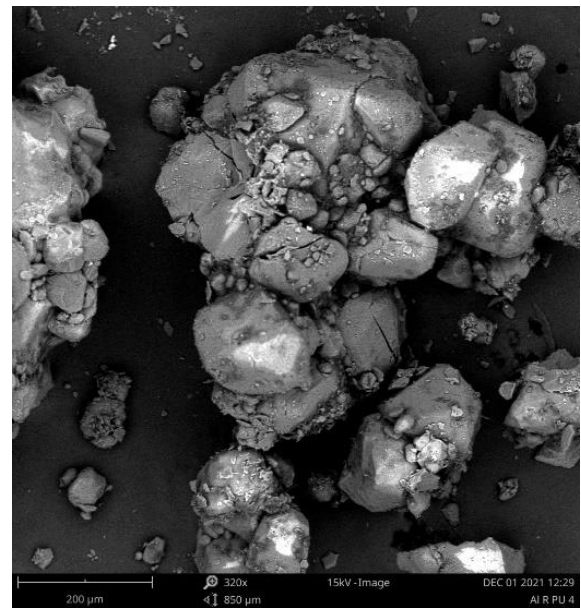
Hexogen	Size/ μm	Circularity	Aspect Ratio	Roundness	Solidity
Uncoated (a)	127.68	0.78	1.47	0.70	0.97
PU-Coated IPDI (b)	96.85	0.87	1.30	0.78	0.98
PU-Coated TDI (c)	64.08	0.78	1.36	0.67	0.98

Infrared spectrometry further identified the polyurethane coating as shown in Figure 3. The figure overlays the infrared spectra of ethyl acetate, HTPB, TDI, hexogen, polyurethane, and coated hexogen. Coated hexogen was free from ethyl acetate as indicated by the

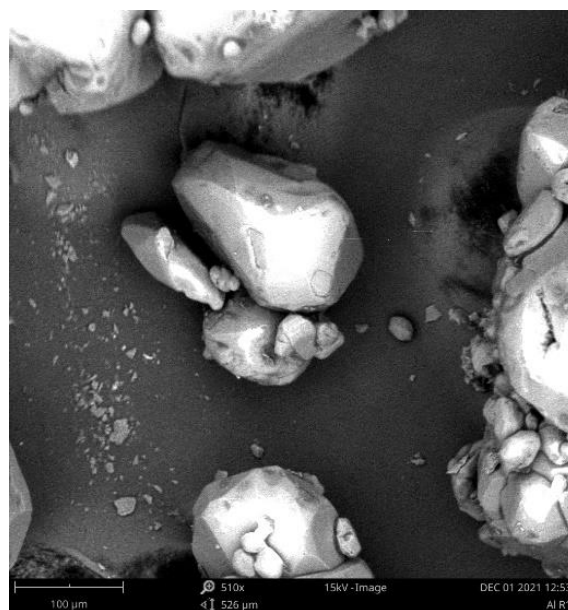
absence of absorption characteristics of the trideuteromethyl and dideuteromethylene at 2300 and 2000 cm^{-1} . The C=O stretching vibration showed progressive displacement at lower frequency with increasing deuteration. The polyurethane formed had both isocyanate and hydroxyl group absorption at 2270 and 3400 cm^{-1} wavelengths. The concentration of the hydroxyl group was difficult to measure, because it had an extensive peak angle quantitatively. Hexogen had infrared characteristic absorption to nitro groups at $1359\text{--}1328\text{ cm}^{-1}$ from the symmetric stretch of the para-nitro group and at $1562\text{--}1535\text{ cm}^{-1}$ assigned to the asymmetric stretch ortho-nitro group [34,35]. The reaction of hexogen with polyurethane produced a diazene oxide group that gave a powerful specific absorption at a wavelength of 2848 and 1758 cm^{-1} [34,35]. The adsorption of isocyanate and diazene oxide can be used to study the kinetic of hexogen coating.



(a)



(b)



(c)

Figure 2. SEM analysis of hexogen (a) and coated hexogen (b,c).

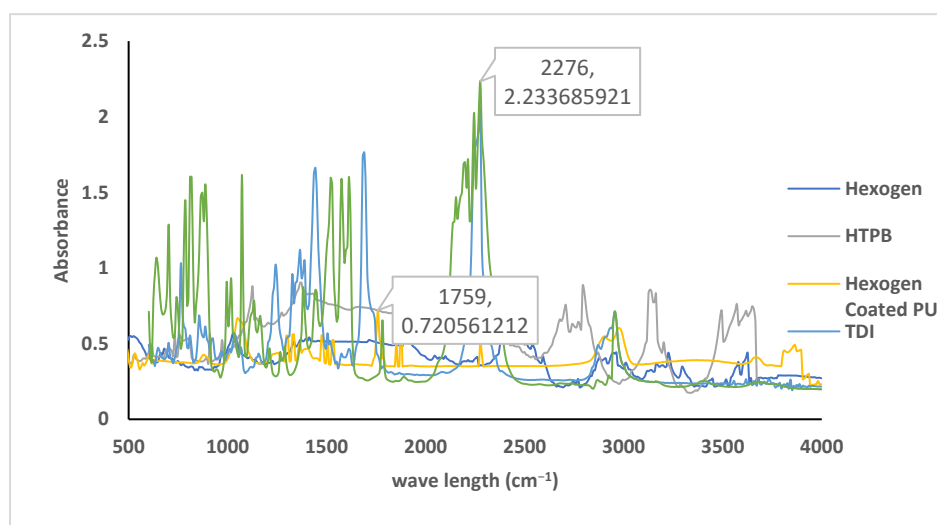


Figure 3. The spectra of ethyl acetate, HTPB, TDI, hexogen, and coated hexogen.

3.2. The Measurement of Isocyanate and Diazene Oxide Concentration

The concentration of isocyanate solution was analyzed by plotting the infrared absorbance at a wavelength of 2276 cm^{-1} and extrapolation to the isocyanate calibration curve. Quantitative infrared spectroscopy analysis applied a standard liquid cuvet sampler for the Prestige FTIR diameter of 1 cm. The conversion of the absorbance to the concentration used the Beer law, in which the spectra absorbance is linear to their concentration if the other parameters are constant. Figure 4 illustrates the isocyanate calibration curve, where the absorbance value was linear to their isocyanate concentration and was expressed by the equation $\text{Abs} = 0.1726\text{ CNCO} - 0.0053$ with an R^2 value = 0.9986. These linear relationships showed no significant interference and could be used for quantitative analysis.

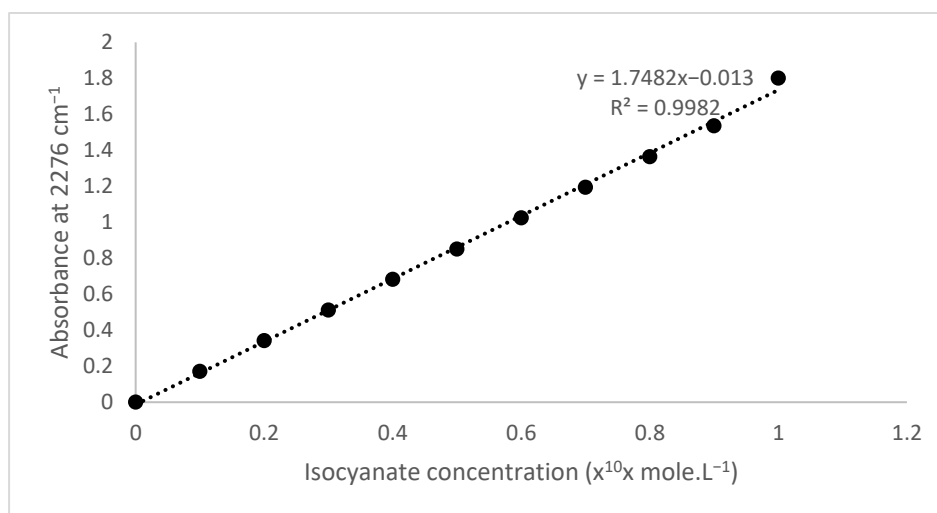


Figure 4. The isocyanate calibration curve based on TDI spectra.

The diazene solution concentration was analyzed by plotting the infrared absorbance at a wavelength of 1768 cm^{-1} and extrapolation to the diazene calibration curve. Quantitative infrared spectroscopy analysis used a standard liquid cuvet sampler for the Prestige FTIR diameter of 1 cm. The conversion of the absorbance to the concentration used the Beer law, where the spectra's absorbance was linear to their concentration if the other parameters were constant. The diazene calibration curve is illustrated in Figure 5, and shows that the absorbance value was linear to their diazene concentration and is expressed by equation $\text{Abs} = 16.066\text{ CNCO} - 0.1247$ with an R^2 value = 0.9973.

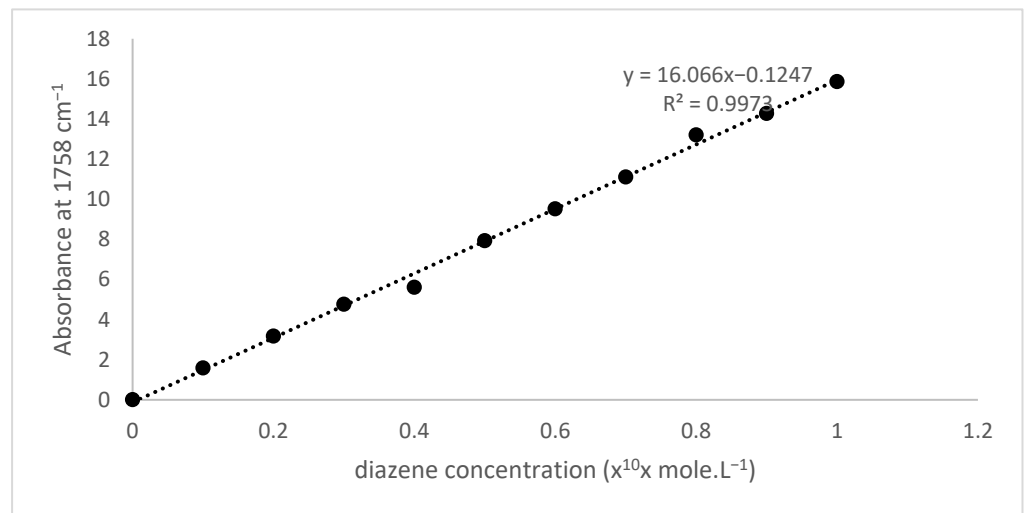


Figure 5. The diazene calibration curve based on 4,4,4'-dimethoxyazoxybenzene spectra.

3.3. Kinetic Evaluation

The coating kinetics of hexogen and polyurethane-based HTPB were evaluated based on the infrared absorbance at 2276 (specific absorption for isocyanate group) [15,21] and 1758 cm^{-1} (specific absorption for diazene oxide group) as a reference [34,35]. The absorbance of the sample was fitted to the calibration curve and converted to their concentrations. In order to study the kinetic model, the isocyanate and diazene oxide concentrations were plotted to the time reaction as seen in Figure 6. The decreasing isocyanate concentration meant that HTPB reacted with TDI, while the increasing diazene concentration indicated the reaction between hexogen and polyurethane.

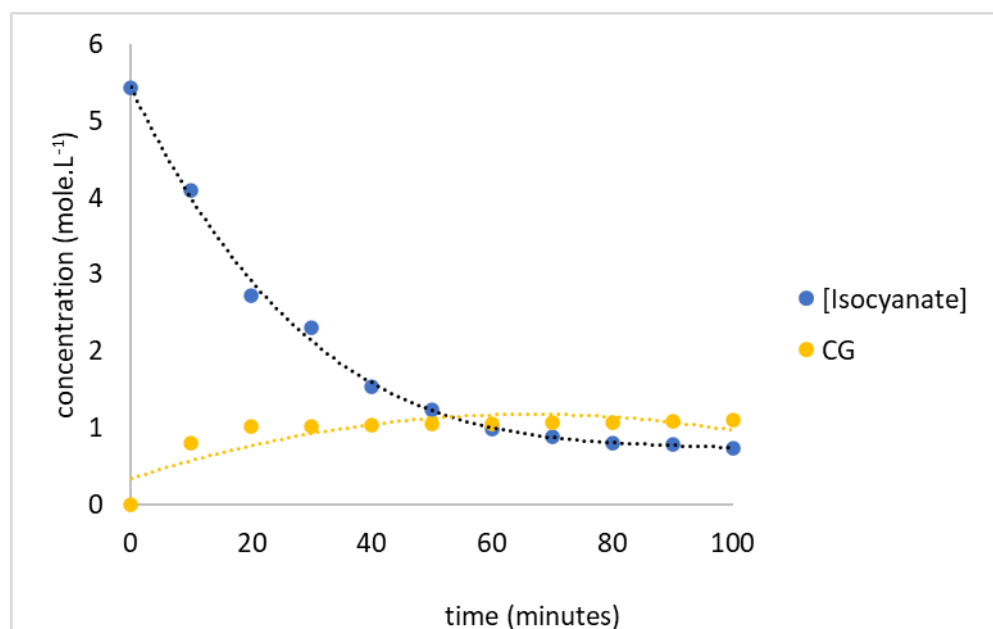


Figure 6. The decreasing isocyanate concentration and increasing diazene oxide concentration following hexogen coating with TDI.

The kinetics model was evaluated through reaction steps including (1) hydroxyl group (A) and isocyanate group (B) to produce urethane group (D), (2) urethane group (D) and isocyanate group (B) to produce allophanate group (E), and (3) nitro group (F) and isocyanate group (B) to produce diazene oxide group (G) and carbon dioxide (H). The car-

bon dioxide (gas) was removed from the reactor. Hence, the reactions can be shown in Equations (4)–(6) with reaction rate constants k_1 , k_2 , and k_3 .



Each step was assumed to fit the first-order reaction with the rate constant of k_1 , k_2 , and k_3 . The reactivity of the functional groups in solution did not depend on their molecular size. The decreasing concentration rate of A was expressed by Equation (7), while the decreasing concentration rates of B, D, and F were shown in Equations (8)–(10) based on the increasing concentration of G.

$$-dC_A/dt = k_1 C_A C_B \quad (7)$$

$$-dC_B/dt = k_1 C_A C_B + k_2 C_D C_B - k_3 C_G \quad (8)$$

$$-dC_D/dt = -k_1 C_A C_B + k_2 C_D C_B \quad (9)$$

$$-dC_F/dt = dC_G/dt = k_3 C_G \quad (10)$$

The diazene oxide formation rate in Equation (10) was independent of the other equations. The integration of Equation (10) with initial $C_{G0} = 0$ at $t = 0$ gave relation C_G to time (t) in Equation (11). The diazene oxide formation rate constant, k_3 , was calculated from the $\ln C_G$ versus t curve slope as shown in Figure 7. The calculated k_3 was $9.11 \times 10^{-4} \text{ L mole}^{-1} \cdot \text{min}^{-1}$.

$$\ln C_G = k_3 t \text{ or } C_G = e^{k_3 t} \quad (11)$$

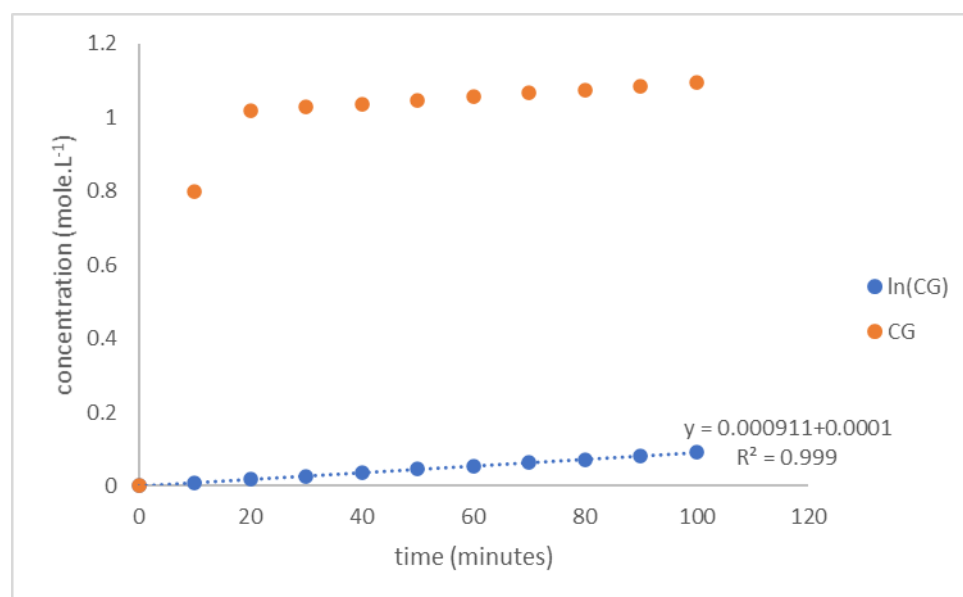


Figure 7. Curve $\ln C_G$ versus t of hexogen coating with TDI.

Equations (12) and (13) show the mole balance of hydroxyl groups (A) and isocyanate groups (B) at a specific reaction time, where C_{A0} and C_{B0} are the initial concentration of A and B, respectively.

$$C_{A0} = C_A + C_D + C_E \quad (12)$$

$$C_{B0} = C_B + C_D + 2C_E + C_G \quad (13)$$

Substitution of Equation (12) into Equation (13) can derive C_E and C_D as a function of C_A and C_B such as the Equations (14) and (15):

$$C_E = C_{B0} - C_{A0} + C_A - C_B - C_G \quad (14)$$

$$C_D = 2C_{A0} - C_{B0} - 2C_A + C_B + C_G \quad (15)$$

Equations (11), (14), and (15) were substituted into Equation (8) to give the decrease of B as a function of C_A, C_B, and C_G:

$$-dC_B/dt = k_1 C_A C_B + k_2 C_B (2C_{A0} - C_{B0} - 2C_A + C_B + e^{k_3 t}) - k_3 e^{k_3 t} \tag{16}$$

There are two reaction rate equations (i.e., Equations (7) and (16)) with the reaction rate constants k₁ and k₂. The initials of C_A and C_B at t = 0 were C_{A0} and C_{B0}. The data source was the isocyanate groups' concentration every ten minutes as seen in Table 2. Equations (7) and (16) were simultaneously nonlinear differential equations. There are two differential equations with three unknown variables (i.e., C_A, k₁, and k₂); thus, the unknown variable can be numerically calculated or estimated using the Newton–Raphson approach. The trial variable was k₁. Initially, k₁ was set to 0.00001 following the value reaction rate constant of polyurethane formation based on the HTPB and TDI [15].

Table 2. The calculated and data C_B every ten minutes.

t (min)	Calculated C _B	Data C _B
0	0.000543	0.000543
10	0.000410	0.000409
20	0.000273	0.000272
30	0.000203	0.000203
40	0.000154	0.000154
50	0.000098	0.000097
60	0.000088	0.000088
70	0.000081	0.000081
80	0.000078	0.000077
90	0.000074	0.000074
100	0.000073	0.000073

Reaction rate equations had the initial isocyanate and hydroxyl groups concentration (t = 0), namely, C_{A0} and C_{B0}. The isocyanates concentration data every ten minutes were expressed by C_{B_i}^d, where i was time. Equations (7) and (16) were numerically solved with the Newton–Raphson method. Equations (7) and (16) were converted to the nonlinear equations of F₁(k₁,k₂) and F₂(k₁,k₂) with the estimated variables k₁ and k₂ following Equations (17) and (18).

$$F_1(k_1, k_2) = dC_A/dt \tag{17}$$

$$F_2(k_1, k_2) = dC_B/dt \tag{18}$$

Initially, variables k₁ and k₂ were set, then the new k₁ and k₂ were estimated by Equations (19) and (20), with n being the iteration increment.

$$k_{1_{n+1}} = k_{1_n} + \frac{-F_1(k_{1_n}, k_{2_n}) \frac{\partial F_2}{\partial k_2} + F_2(k_{1_n}, k_{2_n}) \frac{\partial F_1}{\partial k_2}}{\frac{\partial F_1}{\partial k_1} \frac{\partial F_2}{\partial k_2} + \frac{\partial F_2}{\partial k_1} \frac{\partial F_1}{\partial k_2}} \tag{19}$$

$$k_{2_{n+1}} = k_{2_n} + \frac{-F_1(k_{1_n}, k_{2_n}) \frac{\partial F_2}{\partial k_1} + F_2(k_{1_n}, k_{2_n}) \frac{\partial F_1}{\partial k_1}}{\frac{\partial F_1}{\partial k_1} \frac{\partial F_2}{\partial k_2} + \frac{\partial F_2}{\partial k_1} \frac{\partial F_1}{\partial k_2}} \tag{20}$$

The k₁ and k₂ were continuously iterated until a tolerance boundary error was achieved. The tolerance boundary error was achieved by the least squares error (SSE) and expressed in Equation (21).

$$\sum_{i=1}^{10} |C_{B10i}^d - C_{B10i}^c|^2 \leq tol \tag{21}$$

The value of $\frac{\partial F_1}{\partial x}$, $\frac{\partial F_2}{\partial x}$, $\frac{\partial F_1}{\partial y}$, and $\frac{\partial F_2}{\partial y}$ was approached by the function value difference from k_{1_n} + ε to k_{1_n}, where ε → 0, expressed by Equations (22)–(25).

$$\frac{\partial F_1}{\partial k_2} = \frac{F_1(k_{1_n}, k_{2_n} + \epsilon) - F_1(k_{1_n}, k_{2_n})}{\epsilon} \tag{22}$$

$$\frac{\partial F_1}{\partial k_1} = \frac{F_1(k_{1n} + \epsilon, k_{2n}) - F_1(k_{1n}, k_{2n})}{\epsilon} \quad (23)$$

$$\frac{\partial F_2}{\partial k_2} = \frac{F_1(k_{1n}, k_{2n} + \epsilon) - F_1(k_{1n}, k_{2n})}{\epsilon} \quad (24)$$

$$\frac{\partial F_2}{\partial k_1} = \frac{F_1(k_{1n} + \epsilon, k_{2n}) - F_1(k_{1n}, k_{2n})}{\epsilon} \quad (25)$$

The Runge–Kutta method numerically solved the simultaneous differential equations of F_1 and F_2 . Equations (7) and (16) can be symbolized by $dC_A/dt = f_1(t, C_A, \text{ and } C_B)$ and $dC_B/dt = f_2(t, C_A, \text{ and } C_B)$ with a known value of k_1 and k_2 . The values of C_A and C_B were iterations calculated by increasing t from $t = 0$ to $t = N$. Higher incremental values number will increase their accuracy. In this calculation, number N was set to 10,000. The initial iteration was t_0 , then $t_1 = t_0 + \Delta t$, $t_2 = t_1 + \Delta t$, until $t_{n+1} = t_n + \Delta t$. The C_A and C_B at $t = 0$ were C_{A0} and C_{B0} . The next C_A and C_B were calculated by intermediate constants l_1, l_2, l_3 , and l_4 for function F_1 and intermediate constants m_1, m_2, m_3 , and m_4 for function F_2 following Equations (26)–(35). The calculation of C_A and C_B were iterated until the $t = t_N$. Initially, t was set at 0–10 min; then, this calculation was repeated, where the t was set at 20, 30, 40, . . . , until 100. Thus, the calculated C_A and C_B values at $t = 0, 10, 20, \dots$ until 100 were recorded as C_{Ai} and C_{Bi} . The value of C_{Bi} contributed to calculating the SSE.

$$l_1 = f_1(t_n, C_{A_n}, C_{B_n})\Delta t \quad (26)$$

$$m_1 = f_2(t_n, C_{A_n}, C_{B_n})\Delta t \quad (27)$$

$$l_2 = f_1\left(t_n + \frac{\Delta t}{2}, C_{A_n} + \frac{k_1}{2}, C_{B_n} + k_1/2\right)\Delta t \quad (28)$$

$$m_2 = f_2\left(t_n + \frac{\Delta t}{2}, C_{A_n} + \frac{k_1}{2}, C_{B_n} + k_1/2\right)\Delta t \quad (29)$$

$$k_3 = f_1(t_n + \Delta t/2, C_{A_n} + k_2/2, C_{B_n} + k_2/2)\Delta t \quad (30)$$

$$l_3 = f_2(t_n + \Delta t/2, C_{A_n} + l_2/2, C_{B_n} + l_2/2)\Delta t \quad (31)$$

$$k_4 = f_1(t_n + \Delta t/2, C_{A_n} + k_3/2, C_{B_n} + k_3/2)\Delta t \quad (32)$$

$$l_3 = f_2(t_n + \Delta t/2, C_{A_n} + l_3/2, C_{B_n} + l_3/2)\Delta t \quad (33)$$

$$k_4 = f_1(t_n + \Delta t, C_{A_n} + k_3, C_{B_n} + k_3)\Delta t \quad (34)$$

$$l_4 = f_2(t_n + \Delta t, C_{A_n} + l_3, C_{B_n} + l_3)\Delta t \quad (35)$$

$$C_{A_{n+1}} = C_{A_n} + (k_1 + k_2 + k_3 + k_4)/6 \quad (36)$$

$$C_{B_{n+1}} = C_{B_n} + (k_1 + k_2 + k_3 + k_4)/6 \quad (37)$$

In this calculation, the error tolerance was set to $\text{tol} = 0.00001$, $\epsilon = 0.000001$, $\Delta t = 0.001$, and $N = 10,000$. Initially, the isocyanate and hydroxyl concentrations were $C_{A0} = C_{B0} = 5.43 \text{ moles L}^{-1}$. The initially estimated k_1 and k_2 were 0.000001, following the reaction rate constant of polyurethane formation at bulk and solution conditions [15,20].

From the calculation, the reaction rate constants of k_1 and k_2 were 6.02×10^{-4} and $3.08 \times 10^{-4} \text{ L mole}^{-1} \cdot \text{min}^{-1}$. Overall, the k_1, k_2 , and k_3 values were 6.02×10^{-4} , 3.08×10^{-4} , and $9.11 \times 10^{-4} \text{ L mole}^{-1} \cdot \text{min}^{-1}$, respectively.

The value of $k_2 \ll k_1$ means the branch bonding formation rate was lower than the linear bonding one. The value of k_1 represents the rate constant of a simpler reaction approach of HTPB and TDI as previously reported by Ajithkumar et al. [19] and Wibowo et al. [21,47] in which the polymerization rate constant in a solution at ambient temperature with the initial mole ratio of NCO to OH (RNCO/OH) 1:1 is $6.0 \times 10^{-4} \text{ L mole}^{-1} \cdot \text{min}^{-1}$. This reaction rate is faster than in the bulk system reported by Wibowo [21], Lucio et al. [48], and Olejnik et al. [49]. The value $k_3 \gg k_1 \gg k_2$ represents that the diazene oxide bonding formation rate is faster than the urethane and allophanate bonding formation. Generally,

the reactivity of nitro groups is higher than hydroxyl or urethane groups. The negative partial charge of the O atom of nitro groups is higher than that of the O atom of hydroxyl groups; thus, nitro groups are more reactive than hydroxyl groups. The coating reaction of hexogen with polyurethane is faster than copolymerization of HTPB and TDI. Initially, each isocyanate groups of TDI react with the nitro group of hexogen; then, the other isocyanate groups of TDI react with hydroxyl to produce urethane.

3.4. Effect of the Reaction Temperature

The effect of temperature on the reaction rate constant was presented with the Arrhenius relation, shown in Equation (14), where k_i , A_i , E_i , R , and T are the reaction rate constant in reaction step- i ($i = 1, 2, 3$), collision factor in reaction step i , activation energy in reaction step i , ideal gas constant, and reaction absolute temperature, respectively.

$$k_i = A_i e^{(-E_i/RT)} \quad (38)$$

The reaction temperature significantly affects the coating and polymerization rate following the Arrhenius equation as presented in Equation (14) [30]. After the reaction rate constant (k_i) was calculated, $\ln(k_i)$ was plotted versus $(1/T)$, and the linear regression was analyzed as seen in Figure 8. The graphic intercept was $\ln(A)$, and the slope was $(-E_i/R)$. The calculated activation energy of reaction rate constants E_1 , E_2 , and E_3 were 1178 kJ mol^{-1} , 1021 kJ mol^{-1} , and 912 kJ mol^{-1} . The regression coefficients (R^2 value) were 0.9818, 0.9678, and 0.9560. The effect of the reaction temperature was more significant for a branch bonding than a linear bonding formation, although it had a lower reaction rate constant following $E_1 > E_2 > E_3$. The first reaction was more sensitive to the change in the reaction temperature. The diazene oxide formation was faster and more sensitive to the reaction temperature than the polyurethane formation. The linear bonding formation was more sensitive to the rising temperature than the branch bonding one. The lower value of activation energy supports this phenomenon. This value was similar to the polymerization of HTPB-TDI at the bulk system reported earlier with the value of activation energy 1152 and 1001 kJ mol^{-1} [25,28].

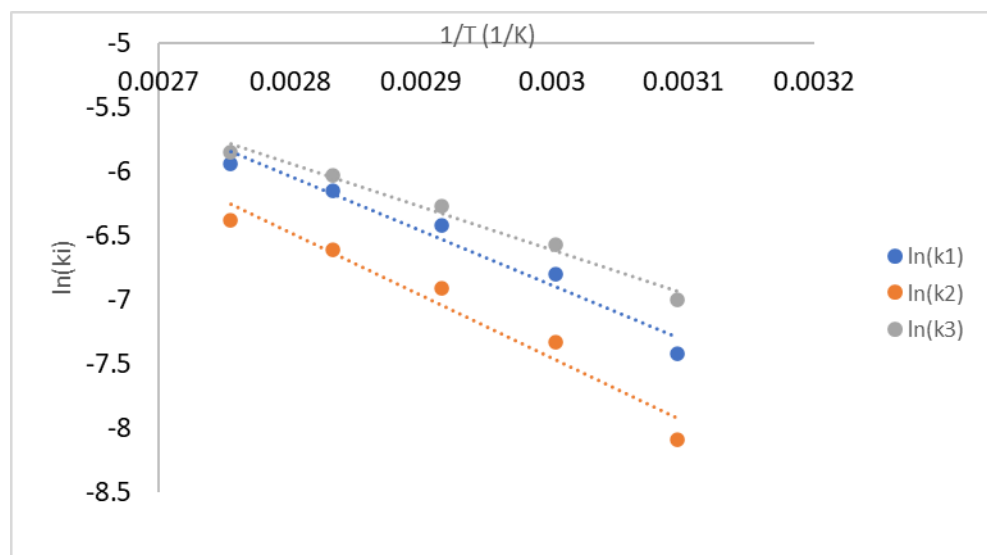


Figure 8. The plot of $\ln(k_i)$ vs. $1/T$ for hexogen coating with polyurethane.

3.5. Kinetics Evaluation of IPDI

Coating kinetics of hexogen and polyurethane-based HTPB was evaluated using IPDI as a curing agent. The isocyanate and diazene oxide concentrations equivalent to the absorbance spectra at 2276 and 1758 cm^{-1} were plotted to time using a calibration curve of isocyanate and diazene oxide concentrations as illustrated in Figures 4 and 5 [20]. The decreasing absorbance meant that the hexogen and HTPB reacted with IPDI. The decreasing

isocyanate concentration and the increasing diazene oxide concentration every ten minutes is presented in Figure 9. The decreasing isocyanate concentration followed by the increasing diazene oxide shows that the hexogen was coated with polyurethane. In this case, the running reaction significantly reduced the isocyanate concentration and increased the diazene oxide concentration. The reaction proceeded very slowly for the first 60 min and tended to be constant. The profile of the decreasing isocyanate concentration followed a polynomial-like shape because of the differential Equations (7)–(10).

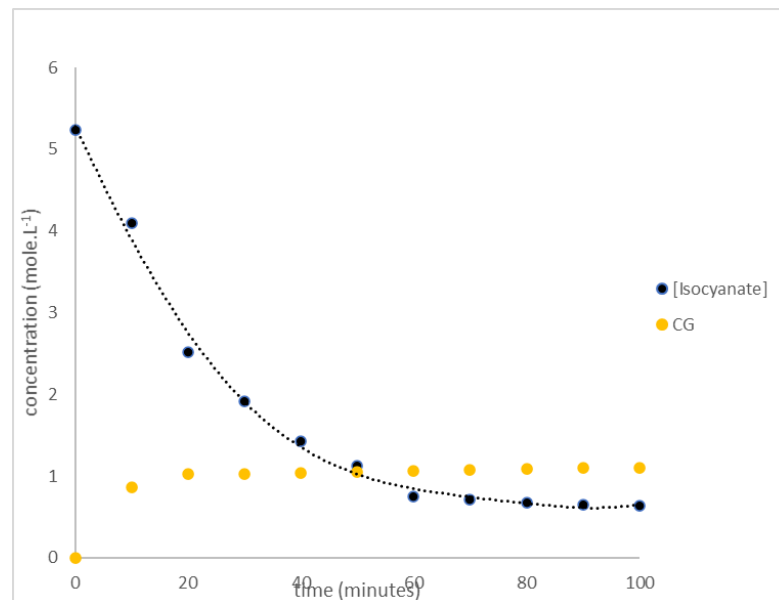


Figure 9. The decreasing isocyanate concentration and increasing diazene oxide concentration following hexogen coating with IPDI.

The reaction rate constants, k_1 and k_3 , were calculated numerically with the Newton–Raphson method, and the simultaneous differential Equations (7) and (16) were solved numerically using the Runge–Kutta method, as expressed in Equation (20)–(27). The kinetic model was evaluated by solving the simultaneous equations in Equations (7)–(10), similar to the TDI process with a tolerance error of 0.0001. The reaction rate constant, k_3 , was measured by plotting $\ln C_G$ vs. t as illustrated in Figure 10. The calculated k_3 is the slope of this graphic, which was $10.04 \times 10^{-4} \text{ L mole}^{-1} \cdot \text{min}^{-1}$.

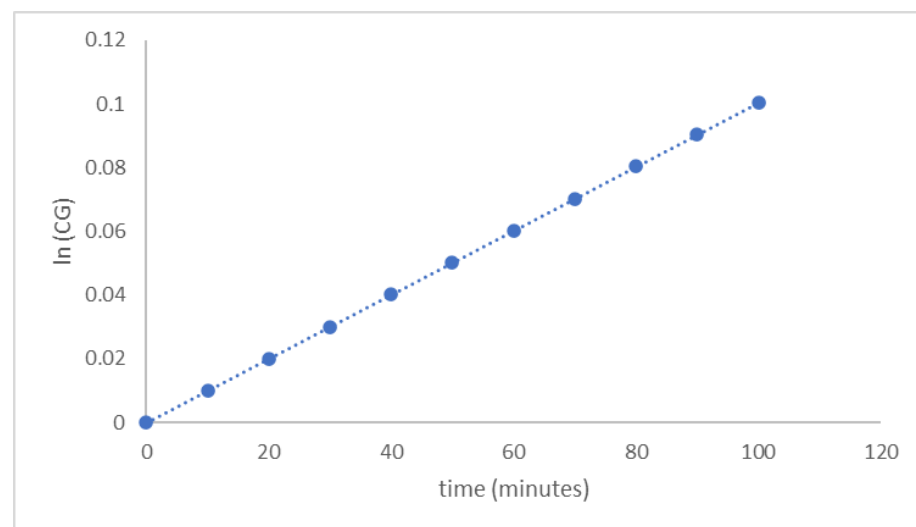


Figure 10. The curve $\ln C_G$ vs. t of hexogen coating with IPDI.

The calculated reaction rate constants k_1 , k_2 , and k_3 were 7.58×10^{-4} , 6.89×10^{-4} , and $10.04 \times 10^{-4} \text{ L mol}^{-1} \text{ min}^{-1}$. The reaction rate constant (k_i) was calculated, $\ln(k_i)$ was plotted versus $(1/T)$, and the linear regression was analyzed as seen in Figure 11. The graphic slope was $(-E_i/R)$, the activation energy E_1 , E_2 , and E_3 were 1008, 959, and 724 kJ mol^{-1} . The regression coefficients (R^2 value) were 0.9909, 0.9848, and 0.9936. The reaction rate of IPDI was slightly faster than that of TDI. This finding is similar to the kinetic investigation by Zhang et al. and Kamran et al. [29,31] in separate research. The reactivity of isocyanate groups in TDI was more stable than that in IPDI because of the resonance between CH_2 groups in the aromatic benzene structure [50,51]. This phenomenon resembles polyurethane polymerization from HTPB with several isocyanates in the extrusion process [50].

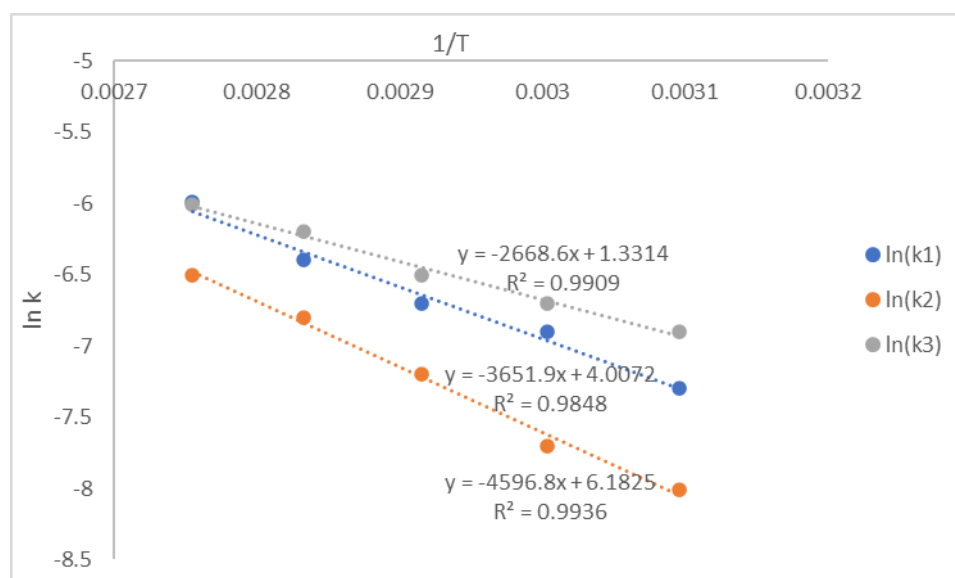


Figure 11. The plot of $\ln(k_i)$ versus $1/T$ for hexogen coating with polyurethane-based IPDI.

Generally, the kinetic value of hexogen coating with IPDI was similar to that of hexogen with TDI. The branch bonding formation rate was lower than the linear bonding one, and the coating reaction of hexogen was faster than their copolymerization. Therefore, all urethane formed reacted constantly with hexogen to produce a diazene oxide bond.

4. Conclusions

Hexogen coating with polyurethane-based HTPB can be identified from the growth in particle size and sphericity. The coating can be observed from decreasing isocyanate and increasing diazene oxide concentrations using infrared spectroscopy following their absorption at 2276 and 1758 cm^{-1} . Moreover, the quantitative analysis was conducted by plotting the absorbance of a particular wavelength on the calibration curve. The evaluation of the kinetics model consisted of several steps: (1) a hydroxyl group and an isocyanate group to produce a urethane group, (2) a urethane group and an isocyanate group to produce an allophanate group, and (3) a nitro group and an isocyanate group to produce a diazene oxide group and carbon dioxide. The constant reaction rate, k_3 , was calculated based on the increasing diazene oxide concentration. The reaction rate constants, k_1 and k_2 , were numerically calculated using the Newton–Raphson and Runge–Kutta methods based on the decreasing isocyanate concentration. Calculation of the reaction rate constants using the kinetics model developed at an initial mole ratio of isocyanate to hydroxyl group 1:1 generated k_1 , k_2 , and k_3 values of 6.02×10^{-4} , 3.08×10^{-4} , and $9.11 \times 10^{-4} \text{ L mol}^{-1} \text{ min}^{-1}$, respectively. In addition, the activation energy of those steps was 1178, 1021, and 912 kJ mol^{-1} . There was a slightly different reaction rate constant of hexogen coated with IPDI and TDI. The reaction rate of hexogen coated with IPDI was

faster than that coated with TDI. The reaction rate constants k_1 , k_2 , and k_3 were 7.58×10^{-4} , 6.89×10^{-4} , and $10.04 \times 10^{-4} \text{ L mol}^{-1} \text{ min}^{-1}$. Meanwhile, the activation energy E_1 , E_2 , and E_3 were 1008, 959, and 724 kJ mol^{-1} .

Author Contributions: Conceptualization, H.B.W.; methodology, H.B.W.; software, H.R.D.S.; validation, H.B.W. and H.R.D.S.; formal analysis, H.R.D.S.; investigation, H.R.D.S. and R.S.B.; resources, R.S.M.W.; data curation, H.B.W.; writing—review and editing, K.H., L.H.A., R.A., H.B.W. and H.R.D.S.; visualization, H.R.D.S. and R.S.M.W.; supervision, H.B.W.; project administration, H.B.W.; funding acquisition. The main contributors were H.B.W. and H.R.D.S. All authors have read and agreed to the published version of the manuscript.

Funding: The authors would like to express their gratitude to the Rispero-LPDP Fund Program Batch-II through the Competitive Research RISPRO-LPDP Program Batch II for financial support in conducting this research with contract No. 082.01.06.3534.001.002.053A.524119 and Skep-27/LPDP/2020.

Institutional Review Board Statement: Not applicable.

Informed Consent Statement: Not applicable.

Data Availability Statement: The data presented in this study are available upon request from the corresponding author.

Acknowledgments: The authors would like to convey our gratitude towards Rocket Technology Center, Rispero-LPDP, and Dahana Co., Ltd.

Conflicts of Interest: The authors declare that they have no conflict of interest.

References

1. Yano, Y.; Gomi, T. Burning rate characteristics of RDX-CMDB propellants. *J. Jpn. Soc. Aeronaut. Space Sci.* **1986**, *34*, 447–452. [[CrossRef](#)]
2. Damse, R.S.; Singh, A.; Singh, H. High Energy Propellants for Advanced Gun Ammunition Based on RDX, GAP and TAGN Compositions. *Propellants Explos. Pyrotech.* **2007**, *32*, 52–60. [[CrossRef](#)]
3. Wibowo, H.B. Current solid propellant research and development in Indonesia and its future direction. *J. Phys. Conf. Ser.* **2018**, *1130*, 012027. [[CrossRef](#)]
4. Jensen, T.L.; Unneberg, E.; Kristensen, T.E. Smokeless GAP-RDX Composite Rocket Propellants Containing Diaminodinitroethylene (FOX-7). *Propellants Explos. Pyrotech.* **2017**, *42*, 381–385. [[CrossRef](#)]
5. Tong, Y.; Liu, R.; Yang, L.; Zhou, Z.N.; Zhang, T.L.; Wang, W.J. Thermal behaviors of RDX/AP/Al Composite Propellants by DSC and TG. *J. Beijing Inst. Technol. Engl. Ed.* **2014**, *23* (Suppl. S1), 17–22.
6. An, C.; Wang, J.; Xu, W.; Li, F. Preparation and Properties of HMX Coated with a Composite of TNT/Energetic Material. *Propellants Explos. Pyrotech.* **2010**, *35*, 365–372. [[CrossRef](#)]
7. An, C.-W.; Li, F.-S.; Song, X.-L.; Wang, Y.; Guo, X.-D. Surface Coating of RDX with a Composite of TNT and an Energetic-Polymer and its Safety Investigation. *Propellants Explos. Pyrotech.* **2009**, *34*, 400–405. [[CrossRef](#)]
8. Liu, H.; Ao, W.; Hu, Q.; Liu, P.; Hu, S.; Liu, L.; Wang, Y. Effect of RDX content on the agglomeration, combustion and condensed combustion products of an aluminized HTPB propellant. *Acta Astronaut.* **2020**, *170*, 198–205. [[CrossRef](#)]
9. Gan, J.; Zhang, X.; Zhang, W.; Hang, R.; Xie, W.; Liu, Y.; Luo, W.; Chen, W. Research Progress of Bonding Agent and Their Performance Evaluation Methods. *Molecules* **2022**, *27*, 340. [[CrossRef](#)]
10. Dagley, I.J.; Montelli, L.; Parker, R.P.; Silva, V.M. Pressed booster compositions prepared by coating RDX using polymer dispersions. *J. Energ. Mater.* **1992**, *10*, 127–149. [[CrossRef](#)]
11. Mahanta, A.K.; Pathak, D.D. HTPB-Polyurethane: A Versatile Fuel Binder for Composite Solid Propellant. In *Polyurethane*; Zafar, F., Sharmin, E., Eds.; InTech: Rijeka, Croatia, 2012; pp. 229–262. [[CrossRef](#)]
12. Chen, C.Y.; Wang, X.F.; Gao, L.L.; Zheng, Y.F. Effect of HTPB with different molecular weights on curing kinetics of HTPB/TDI system. *Chin. J. Energ. Mater.* **2013**, *21*, 771–776.
13. Chen, J.K.; Brill, T.B. Chemistry and kinetics of hydroxyl-terminated polybutadiene (HTPB) and diisocyanate-HTPB polymers during slow decomposition and combustion-like conditions. *Combust. Flame* **1991**, *87*, 217–232. [[CrossRef](#)]
14. Bina, C.K.; Kannan, K.G.; Ninan, K.N. DSC study on the effect of isocyanates and catalysts on the HTPB cure reaction. *J. Therm. Anal. Calorim.* **2004**, *78*, 753–760. [[CrossRef](#)]
15. Lee, S.; Hong, I.-K.; Lee, J.W.; Jeong, W.B. Rheology and Curing of Hydroxyl Terminated Polybutadiene/(Sugar or Calcium Carbonate) Suspension. *Polym. Korea* **2014**, *38*, 417–424. [[CrossRef](#)]
16. Dubois, C.; Désilets, S.; Ait-Kadi, A.; Tanguy, P. Bulk polymerization of hydroxyl terminated polybutadiene (HTPB) with tolylene diisocyanate (TDI): A kinetics study using ^{13}C -NMR spectroscopy. *J. Appl. Polym. Sci.* **1995**, *58*, 827–834. [[CrossRef](#)]

17. Sultan, W.; Busnel, J.P. Kinetic study of polyurethanes formation by using differential scanning calorimetry. *J. Therm. Anal. Calorim.* **2006**, *83*, 355–359. [[CrossRef](#)]
18. Mahanta, A.K.; Goyal, M.; Pathak, D.D. Rheokinetic Analysis of Hydroxy Terminated Polybutadiene Based Solid Propellant Slurry. *E-J. Chem.* **2010**, *7*, 171–179. [[CrossRef](#)]
19. Ajithkumar, S.; Kansara, S.S.; Patel, N.K. Kinetics of castor oil based polyol–toluene diisocyanate reactions. *Eur. Polym. J.* **1998**, *34*, 1273–1276. [[CrossRef](#)]
20. Li, C.; Luo, T.; Zhang, X.; Liu, J.; Pang, A.; Chi, X. In situ FT-IR spectroscopic studies of curing reaction of HTPB and TDI on solid surface. *J. Shenzhen Univ. Sci. Eng.* **2016**, *33*, 452. [[CrossRef](#)]
21. Wibowo, H.B.; Dharmawan, W.C.; Wibowo, R.S.M. Bulk Polymerization Kinetics of Hydroxy Terminated Polybutadiene and Toluene Diisocyanate with Infrared Spectroscopy. *Indones. J. Chem.* **2018**, *18*, 552. [[CrossRef](#)]
22. Wibowo, H.B.; Wibowo, R.S.M. Non Energetic Binder Application for RDBP Propellant Based Large Caliber Munition (MKB). In Proceedings of the International Seminar on Aerospace Science and Technology IV, Lombok, Indonesia, 20–22 September 2016; pp. 82–91.
23. Wibowo, H.B. Pengaruh gugus hidroksil sekunder terhadap sifat mekanik poliuretan berbasis htpb (hydroxy terminated polybutadiene) (effect of secondary hydroxyl groups on mechanical properties of polyurethane base htpb (hydroxy terminated polybutadiene)). *J. Teknol. Dirgant.* **2015**, *13*, 103–112.
24. Flory, P.J. *Principles of Polymer Chemistry*; Cornell University Press: Ithaca, NY, USA, 1953.
25. Toosi, F.S.; Shahidzadeh, M.; Ramezanzadeh, B. An investigation of the effects of pre-polymer functionality on the curing behavior and mechanical properties of HTPB-based polyurethane. *J. Ind. Eng. Chem.* **2015**, *24*, 166–173. [[CrossRef](#)]
26. Ma, H.; Liu, Y.-C.; Chai, T.; Hu, T.-P.; Guo, J.-H.; Yu, Y.-W.; Yuan, J.-M.; Wang, J.-H.; Qin, N.; Zhang, L. Kinetic studies on the cure reaction of hydroxyl-terminated polybutadiene based polyurethane with variable catalysts by differential scanning calorimetry. *e-Polymers* **2017**, *17*, 89–94. [[CrossRef](#)]
27. Tanver, A.; Huang, M.H.; Luo, Y.J.; Hei, Z.H. Chemical Kinetic Studies on Polyurethane Formation of GAP and HTPB with IPDI by Using In Situ FT-IR Spectroscopy. *Adv. Mater. Res.* **2014**, *1061–1062*, 337–341. [[CrossRef](#)]
28. Guodong, W.; Chai, T.; Liu, Y.; Cui, J.; Ma, H.; Jing, S.; Zhong, L.; Qin, S.; Wang, G.; Ren, X. Kinetic Research on the Curing Reaction of Hydroxyl-Terminated Polybutadiene Based Polyurethane Binder System via FT-IR Measurements. *Coatings* **2018**, *8*, 175. [[CrossRef](#)]
29. Zhang, X.; Liu, Y.; Chai, T.; Ma, Z.; Jia, K. Curing Reaction Kinetics of the EHTPB-Based PBX Binder System and Its Mechanical Properties. *Coatings* **2020**, *10*, 1266. [[CrossRef](#)]
30. Cunliffe, A.V.; Davis, A.; Farey, M.; Wright, J. The kinetics of the reaction of isophorone di-isocyanate with mono-alcohols. *Polymer* **1985**, *26*, 301–306. [[CrossRef](#)]
31. Kamran, P.A.; Kazemini, M. An Experimental Kinetic Investigation of Polymerization of Hydroxyl Terminated Polybutadiene (Htpb) With Isophorone Diisocyanate (Ipdi). *J. Energ. Mater.* **2010**, *4*, 29–38.
32. Valishamekhi, A.; Kebritchi, A.; Kaykha, Y. Investigating the Effect of DBTDL Catalyst on Curing Kinetic of Polyurethane Using Differential Scanning Calorimetry: HTPB/TDI vs. HTPB/IPDI. *J. Appl. Res. Chem.-Polym. Eng.* **2021**, *5*, 43–55. Available online: <https://arce.modares.ac.ir/article-38-44600-en.html> (accessed on 27 December 2021).
33. Tow, G.M.; Maginn, E.J. Cross-Linking Methodology for Fully Atomistic Models of Hydroxyl-Terminated Polybutadiene and Determination of Mechanical Properties. *Macromolecules* **2021**, *54*, 4488–4496. [[CrossRef](#)]
34. Neudorfl, P.S.; Back, R.A.; Douglas, A.E. The absorption spectrum of trans-diimide (N₂H₂) in the vacuum ultraviolet region1. *Can. J. Chem.* **1981**, *59*, 506–517. Available online: www.nrcresearchpress.com (accessed on 26 September 2021). [[CrossRef](#)]
35. Bondybey, V.E.; Nibler, J.W. Infrared and Raman spectra of solid and matrix isolated diimide, HNNH. *J. Chem. Phys.* **1973**, *58*, 2125–2134. [[CrossRef](#)]
36. Joshi, N.; Romanias, M.N.; Riffault, V.; Thevenet, F. Investigating water adsorption onto natural mineral dust particles: Linking DRIFTS experiments and BET theory. *Aeolian Res.* **2017**, *27*, 35–45. [[CrossRef](#)]
37. Bardestani, R.; Patience, G.S.; Kaliaguine, S. Experimental methods in chemical engineering: Specific surface area and pore size distribution measurements—BET, BJH, and DFT. *Can. J. Chem. Eng.* **2019**, *97*, 2781–2791. [[CrossRef](#)]
38. Wibowo, H.B. Isomerisasi polimer melalui reaksi sains sayef untuk mengubah konfigurasi htpb (hydroxyl terminated polybutadiene) polymer isomerization by sains sayef reaction to modify configuration of htpb (hydroxyl terminated polybutadiene). *J. Teknol. Dirgant.* **2016**, *14*, 137–146. [[CrossRef](#)]
39. Krishnan, P.S.G.; Ayyaswamy, K.; Nayak, S.K. Hydroxy Terminated Polybutadiene: Chemical Modifications and Applications. *J. Macromol. Sci. Part A* **2013**, *50*, 128–138. [[CrossRef](#)]
40. Navarchian, A.H.; Picchioni, F.; Janssen, L.P.B.M. Rheokinetics and effect of shear rate on the kinetics of linear polyurethane formation. *Polym. Eng. Sci.* **2005**, *45*, 279–287. [[CrossRef](#)]
41. Kornilov, A.; Safonov, I. An Overview of Watershed Algorithm Implementations in Open Source Libraries. *J. Imaging* **2018**, *4*, 123. [[CrossRef](#)]
42. Lee, S.; Choi, C.H.; Hong, I.-K.; Lee, J.W. Polyurethane curing kinetics for polymer bonded explosives: HTPB/IPDI binder. *Korean J. Chem. Eng.* **2015**, *32*, 1701–1706. [[CrossRef](#)]
43. Fiayyaz, M.; Zia, K.M.; Zuber, M.; Jamil, T.; Khosa, M.K.; Jamal, M.A. Synthesis and characterization of polyurethane/bentonite nanoclay based nanocomposites using toluene diisocyanate. *Korean J. Chem. Eng.* **2014**, *31*, 644–649. [[CrossRef](#)]

44. Betoret, E.; Betoret, N.; Carbonell, J.V.; Fito, P. Effects of pressure homogenization on particle size and the functional properties of citrus juices. *J. Food Eng.* **2009**, *92*, 18–23. [[CrossRef](#)]
45. Argade, P.S.; Magar, D.D.; Saudagar, R.B. Solid Dispersion: Solubility Enhancement Technique for poorly water soluble Drugs. *J. Adv. Pharm. Educ. Res.* **2013**, *3*, 427–439. Available online: www.japer.in (accessed on 20 September 2021).
46. Zdilla, M.J.; Hatfield, S.A.; McLean, K.A.; Cyrus, L.M.; Laslo, J.M.; Lambert, H.W. Circularity, Solidity, Axes of a Best Fit Ellipse, Aspect Ratio, and Roundness of the Foramen Ovale. *J. Craniofac. Surg.* **2016**, *27*, 222–228. [[CrossRef](#)] [[PubMed](#)]
47. Wibowo, H.B.; Dharmawan, W.C.; Wibowo, R.S.M.; Yulianto, A. Kinetic study of htpb (Hydroxyl terminated polybutadiene) synthesis using infrared spectroscopy. *Indones. J. Chem.* **2020**, *20*, 919–928. [[CrossRef](#)]
48. Lucio, B.; de la Fuente, J.L. Rheokinetic analysis on the formation of metallo-polyurethanes based on hydroxyl-terminated polybutadiene. *Eur. Polym. J.* **2014**, *50*, 117–126. [[CrossRef](#)]
49. Olejnik, A.; Gosz, K.; Piszczyk, Ł. Kinetics of cross-linking processes of fast-curing polyurethane system. *Thermochim. Acta* **2020**, *683*, 178435. [[CrossRef](#)]
50. Buchner, G.A.; Rudolph, M.; Norwig, J.; Marker, V.; Gürtler, C.; Schomäcker, R. Kinetic Investigation of Polyurethane Rubber Formation from CO₂-Containing Polyols. *Chem. Ing. Tech.* **2020**, *92*, 199–208. [[CrossRef](#)]
51. Verhoeven, V.W.A.; Padsalgikar, A.D.; Ganzeveld, K.J.; Janssen, L.P.B.M. A kinetic investigation of polyurethane polymerization for reactive extrusion purposes. *J. Appl. Polym. Sci.* **2006**, *101*, 370–382. [[CrossRef](#)]